

APPLICATION OF MICROTEXTURE DETERMINATION USING EBSD TO NON CUBIC CRYSTALS

D J DINGLEY, A DAY and A BEWICK

H H Wills Physics Laboratory, University of Bristol, Tyndall Ave. Bristol BS81TL
UK

INTRODUCTION

The technique for obtaining individual crystal orientation using electron backscatter diffraction (EBSD) in the scanning electron microscope, first demonstrated by Venables and Harland in 1973¹ and adapted for on-line texture determination by Dingley et al. in 1984², is well established for cubic materials, Randle et al.³, Hjelen and Nes⁴, Juul Jensen and Randle⁵. Extension of the technique to hexagonal and rhombohedral crystals was reported briefly by Dingley in 1987^{6,7}. This paper presents a full account of the general procedure for obtaining on-line orientation measurements from non cubic crystals with examples from hexagonal zircaloy and orthorhombic BiSrCuCaO high temperature superconducting material.

It has also been recognised for some time that pole figure representation of the orientation data obtained using the EBSD method is not ideal, and an alternative representation, a Frank Rodrigues (FR) figure, was presented at the 1987 ICOTOM meeting, Frank⁸. Here is presented a further extension of this representation in which the absolute and relative orientations of crystals are displayed in a micrograph of the grain structure by a colour specific to one point in the FR figure.

EXPERIMENTAL PROCEDURE.

Details of the EBSD technique have been published previously Dingley et al.⁹. Briefly, the sample is mounted in an SEM inclined so that its surface normal points 70° from the incident beam and towards a vertical phosphor screen, 50mm in diameter and placed 50 mm from the specimen. To obtain a diffraction pattern the electron beam of the SEM is positioned as a stationary probe within the grain of interest. Kikuchi type diffraction occurs within the specimen and the diffracted beams which exit from the top surface of the specimen are imaged on the phosphor screen. The spatial resolution of the technique is 200nm and the angular precision in orientation measurement 1 to 2, depending on the accuracy of the calibration. The phosphor screen is viewed using a low light level television camera and on-line orientation measurement is made by superimposing onto the TV image of the pattern a computer generated cursor. The cursor is positioned successively on designated zone axes in the pattern and by measuring the locations of these zone axes the pattern can be indexed automatically and the orientation determined. The diffraction pattern centre

and specimen to screen distance, necessary to interpret the patterns, are determined from prior measurements of zone axis positions on a calibration crystal mounted in the microscope at a known orientation. Advances in execution of the technique for cubic crystals have permitted measurement of orientation without the need to input the indices of the selected zone axes, Dingley¹⁰ and in a more advanced technique still the pattern is identified using computer based pattern recognition procedures, Juul Jensen and Schmidt¹¹.

NON-CUBIC CRYSTALS

Diffraction patterns from cubic crystals are relatively easy to recognise because the high symmetry means that each zone axis type is repeated often so that only a few different types need to be remembered by the operator or recognised by the computer. Each is distinguished by the arrangement of Kikuchi lines passing through the zone axis. As the crystal symmetry decreases more zone axes types need to be recognised and whereas this is still relatively simple for hexagonal crystals, distinguishing between $\{100\}$ and $\{001\}$ can become very difficult in orthorhombic crystals for example, especially when the $a:b$ ratio is close to 1. Fig.1 shows a pattern from hexagonal silicon carbide. Indexing is clearly difficult but with the use of a set of reference photographs for a specific crystal structure on-line operator recognition becomes 100% successful. Fig.2 shows a diffraction pattern from the high temperature BiStCuCaO superconducting material taken close to $\{001\}$. The material was prepared by cladding in silver followed by severe cold reduction. Subsequent high temperature annealing in oxygen both recrystallises the material and renders it superconducting. Whereas it was simple to distinguish the $\{001\}$ axis it was not possible to distinguish between $\{100\}$ and $\{010\}$ due to the $a:b$ ratio being 0.01.

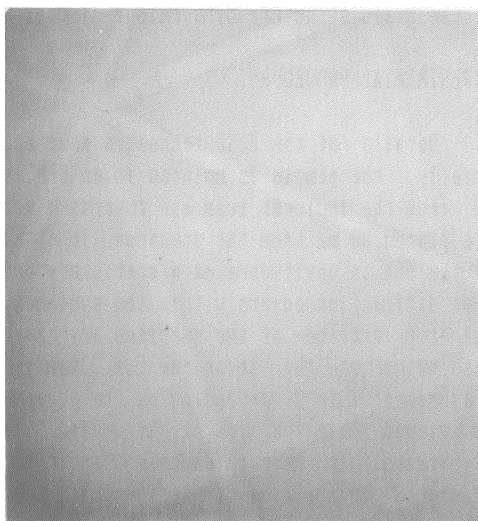
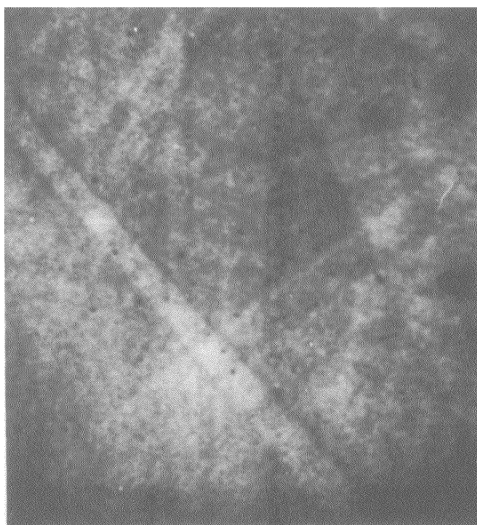


Fig.1 EBSP from hexagonal zirconium alloy

Fig2. EBSP from orthorhombic BiSrCaCuO

RESULTS

On-line orientation measurement of the hexagonal crystals presented no difficulties. Specific zone axes were recognised by the operator. Miller indices of the selected axes were input to the computer and the locations of the axes determined by positioning the computer generated cursor on them. An example of data obtained from annealed zircaloy is presented in the pole figure, fig.3a,b. The basal plane [0001] and pyramidal plane [1010] orientations are shown. The basal plane X-ray determined pole figures for the same specimen are shown in fig.3c,d. for comparison. Considering that only 230 grain orientation were measured to determine the EBSD pole figure the agreement between EBSD and X-ray data is extremely good.

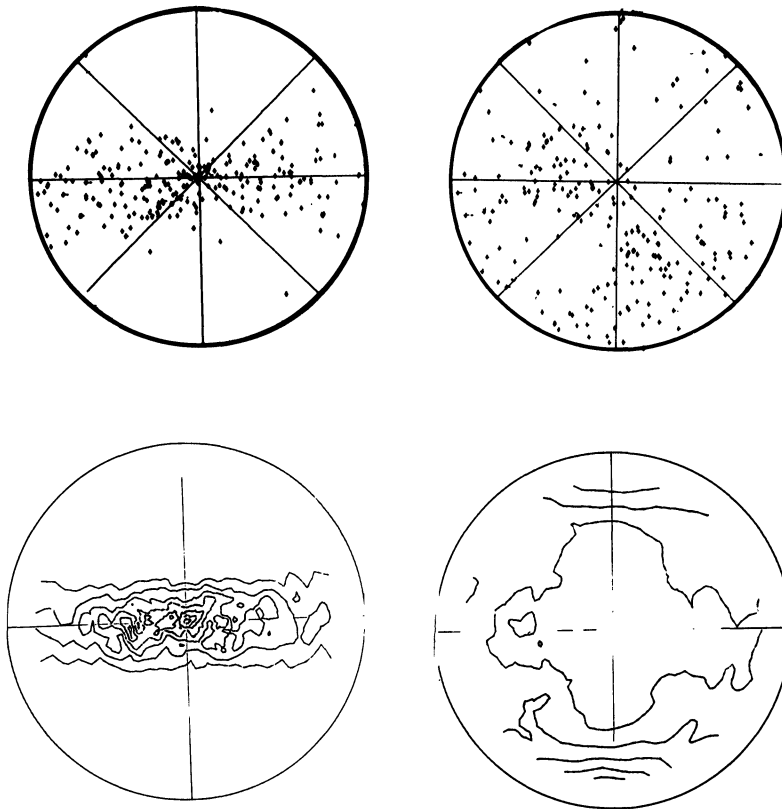


Fig.3. a,b. [0001] and [1010] pole figures for hexagonal zircaloy obtained using EBSD
Fig.3. c,d. Corresponding figures to 3a and 3b obtained using X-ray diffraction

On-line orientation measurement of BiSrCaCuO was more difficult but successful because as the material was highly textured all grains examined presented their [001] axis towards the screen. It was also possible to distinguish on-line between the broad [110] and narrow [010] Kikuchi bands passing through [001]. By adapting the program to accept band positions rather than zone axes, orientation determination could thus be achieved. The results are presented in the pole figure, fig.4a, where the [001] poles only are plotted. The highly textured nature of the material is

shown. Because it was not possible to distinguish between $[100]$ and $[010]$ the data for these two axes are combined in fig.4b.

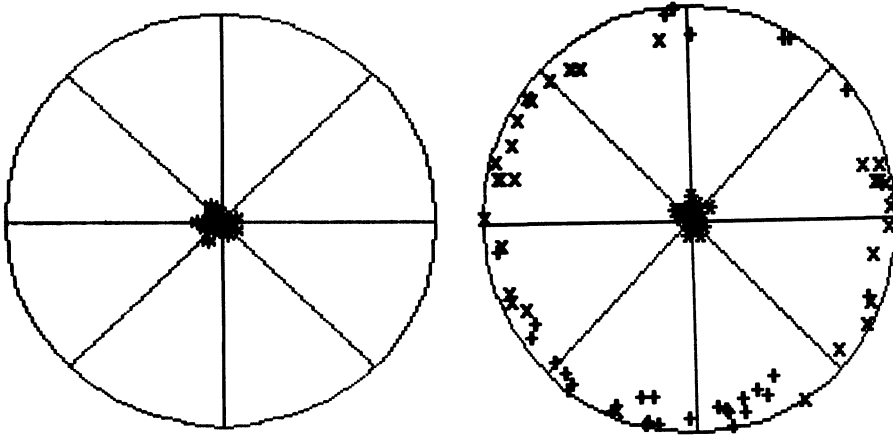


Fig.4. Poles figures obtained using EBSD for BiSrCaCuO . a. $[001]$ poles only.
b. $[001]$, $[100]$ and $[010]$ poles.

FRANK RODRIGUES FIGURES

To determine the absolute orientations of crystals by the combined inspection of figs 3a and 3b or 4a and 4b it is clearly an impossible task. However, the very nature of the EBSD technique provides the absolute orientation of each crystal examined and it is only necessary to produce a means of representing these measurements in pictorial form. A means was described by Frank⁶ which we now refer to as Frank Rodrigues figures. For each crystal the rotation axis and rotation angle are calculated that would rotate the crystal so that its reference axes were made parallel to the reference axes of the specimen. These parameters are given by the Eigen vector and the trace of the orientation matrix respectively defining each crystal. The magnitude of the rotation axis is made equal to the modulus of the vector multiplied by $\tan(\text{half the rotation angle})$. Each vector is plotted in a figure whose origin is the centre of the figure and whose axes are parallel to the specimen reference axes. Such a plot is shown for grain orientations obtained from recrystallised pure nickel in fig.5a. The figure has the advantage that it exhibits the symmetry of the crystal structure and is bounded by a surface also related to the crystal symmetry. Corresponding figures for the zircaloy material is shown in fig.5b

ORIENTATION IMAGING

The combination of scanning electron microscopy and EBSD affords a unique opportunity to represent the spatial distribution of crystal orientations by superimposing on a micrograph of the specimen the individual crystal orientations.

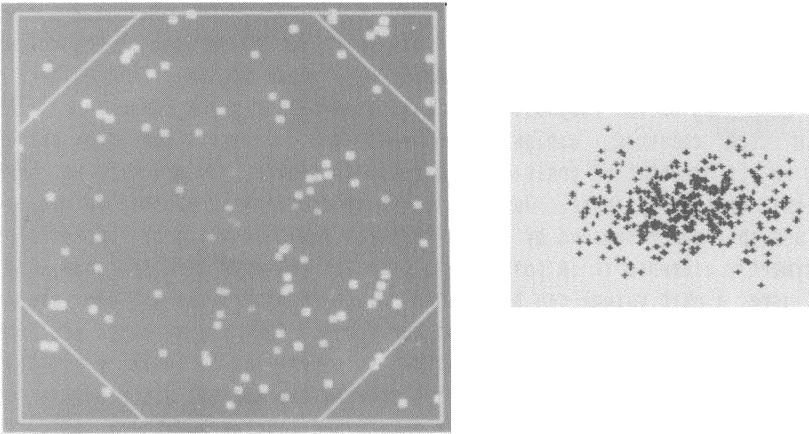


Fig. 5a Rodrigues Frank map for Ni grains. Fig5.b Corresponding map for zircaloy.

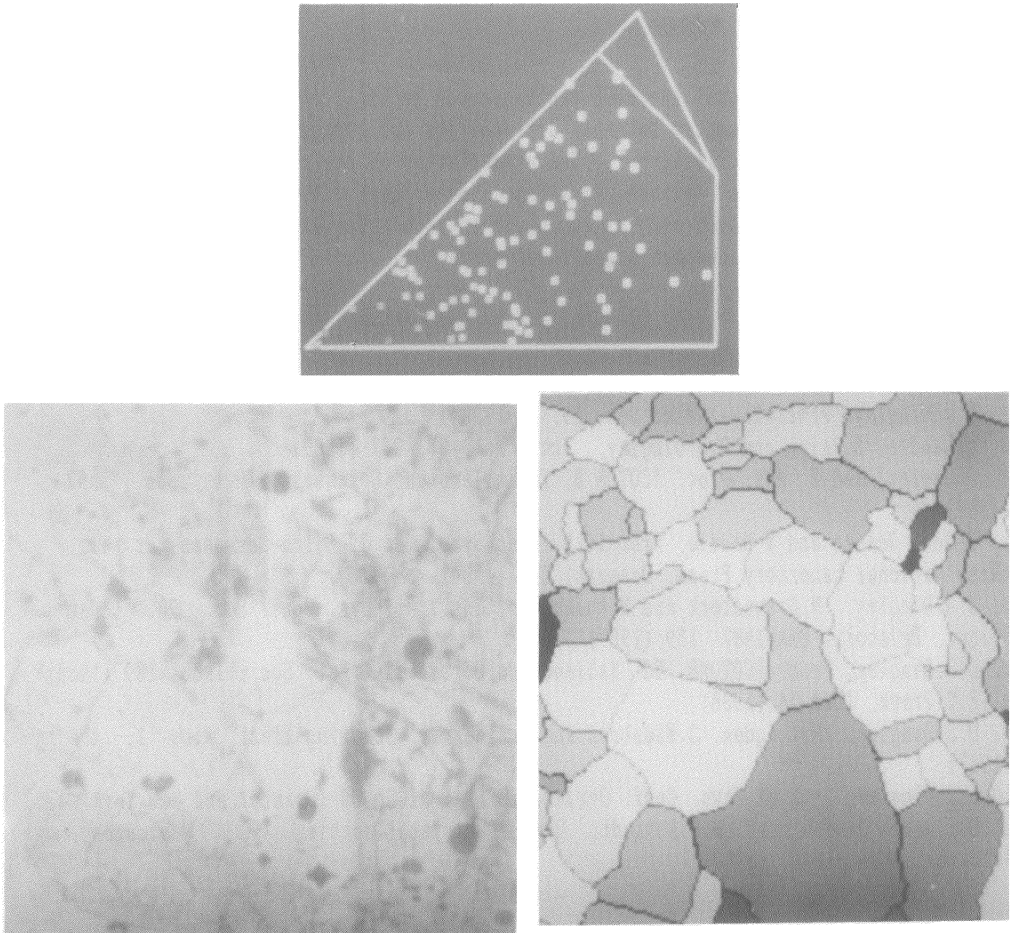


Fig. 6a Ni grain orientations represented in unit volume of FR figure.
Fig. 6b (upper), micrograph of Ni grains, (lower) orientation image of same grains.

As before, the individual orientations are defined in the FR figure. Each x,y,z axis of the figure is assigned the colour red, blue or green, the brightness of the colour increasing with distance from the origin. A point within the figure will then have a unique colour depending on the respective contributions of its x,y,z components. The micrograph is then coloured, assigning to each grain orientation the colour corresponding to its orientation position within the FR figure. In practice we have used a sub-unit of the FR figure. Just as in the stereographic projection it is possible to assign a space bounded by $[001]$, $[110]$, $[111]$ within which by because of the crystal symmetry elements it is possible to transfer all crystal directions, so, in the FR figure, a unit volume can be defined. In this case it is an odd shaped figure, see fig.6. constituting 1/48th. of the total. The x,y,z axes are not orthogonal and the sides are not of equal length. x is parallel to $[001]$, y to $[110]$ and z to $[111]$. Fig.6 also includes a micrograph showing the spatial distribution of the grains from which the orientations were determined together with a coloured superposition of the micrograph and the orientations. It is seen that in this case not only is the texture random but so is the spatial distribution of orientations, i.e. there is no clustering of grains with particular orientations

CONCLUSIONS

It has been shown that the EBSD technique can be extended to include crystals with lower than cubic symmetry but that difficulties and ambiguities can arise where a:b or b:c ratios are close to 1. The presentation of the orientations in Frank Rodrigues map form has obvious advantages over pole figure representation, particularly for non cubics and its extension to permit the imaging of the spatial distribution of orientations has significant merit.

REFERENCES

1. J.A.Venables and C.J.Harland, *Phil. Mag.* 27, 1193 (1973)
2. D.J.Dingley, *Proc. Royal Mic. Soc.* 19, 74 (1984)
3. V.Randle, B.Ralph and D.J.Dingley, *Acta. Met.* 36, 267 (1988)
4. J.Hjelen and E. Nes, *Proc. ICOTOM 8*, Ed Kallend and Gottstein, (*Met. Soc.*) 597 (1988)
5. D.Juul Jensen and V Randle, *Proc 10th. Riso Symp.*, Ed J. Bilde-Sorensen et al., (Riso National Laboratory Press, Denmark) 325 (1984)
6. D.J.Dingley, N.Gravestock and H.Rothstein, *Inst. of Phys. Conf. Ser.* 90. (Adam Hilger, Bristol) EMAG1987 139 (1987)
7. D.J.Dingley, *Proc. ICOTOM8*, Ed. Kallend and Gottstein, (*Met. Soc.*, 1988) 189 (1988)
8. F.C.Frank, *Ibid* 54 (1988)
9. D.J.Dingley, M.Longdon, J.Wienbren and J.Alderman, *Scanning Elect. Mic.* 1, 451 (1987)
- 10 D.J.Dingley, *Inst.of Phys. Conf. Series.* 98 EMAG-MICRO 89 (Bristol and New York) 473, (1989)
- 11 D. Juul Jensen and N.H.Schmidt, *Proc. Recrystallisation '90*, Woolongong, Australia, In press, (1990)